Supporting Information

Pseudocapacitive behaviours of $Na_2Ti_3O_7$@CNT coaxial nanocables for high-performance sodium-ion capacitors

Shengyang Dong, *Laifa Shen*, *Hongsen Li*, *Ping Nie*, *Yaoyao Zhu*, *Qi Sheng and Xiaogang Zhang**

Jiangsu Key Laboratory of Materials and Technology for Energy Conversion, College of Material Science and Engineering, Nanjing University of Aeronautics and Astronautics, Nanjing 210016, P. R. China.

Corresponding author: azhangxg@nuaa.edu.cn (X. G. Zhang)

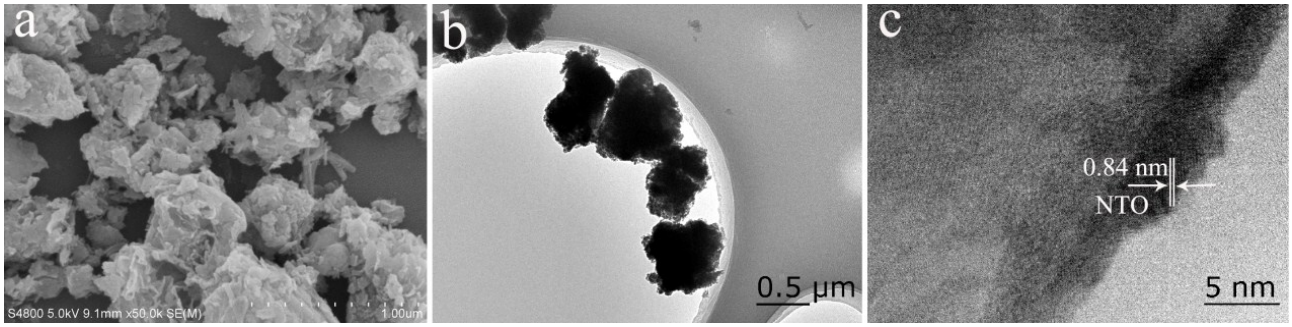

Fig. S1 SEM and TEM images of pristine $Na_2Ti_3O_7$.

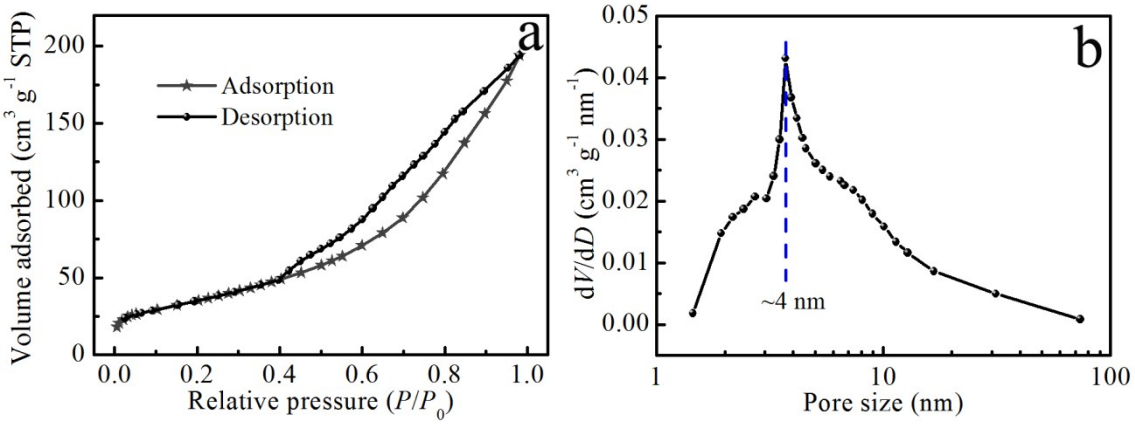

Fig. S2 (a) N_2 adsorption-desorption isotherms of $Na_2Ti_3O_7$@CNT, (b) pore size distribution data through the BJH method.

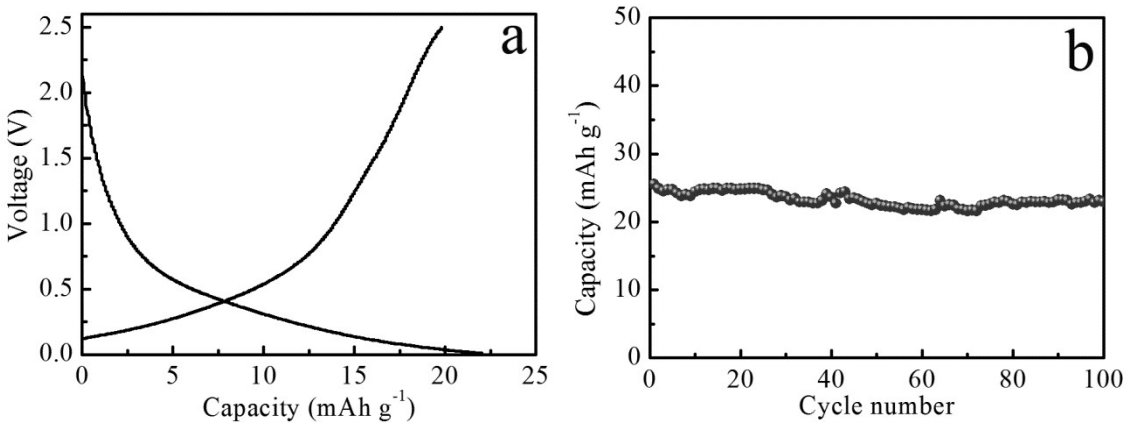

Fig. S3 Charge-discharge voltage profiles and (b) cycling performance at current density of 85 mA g^{-1} of CNTs.

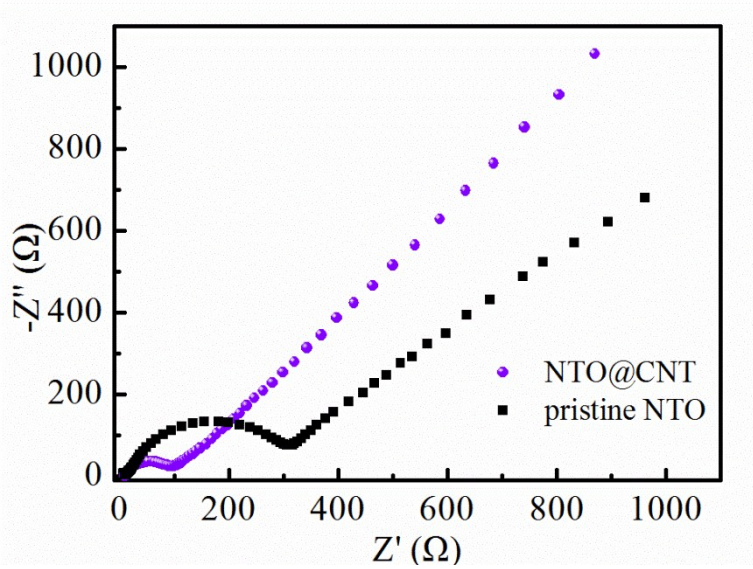

Fig. S4 Nyquist plots of $Na_2Ti_3O_7$@CNT and pristine $Na_2Ti_3O_7$ electrodes.

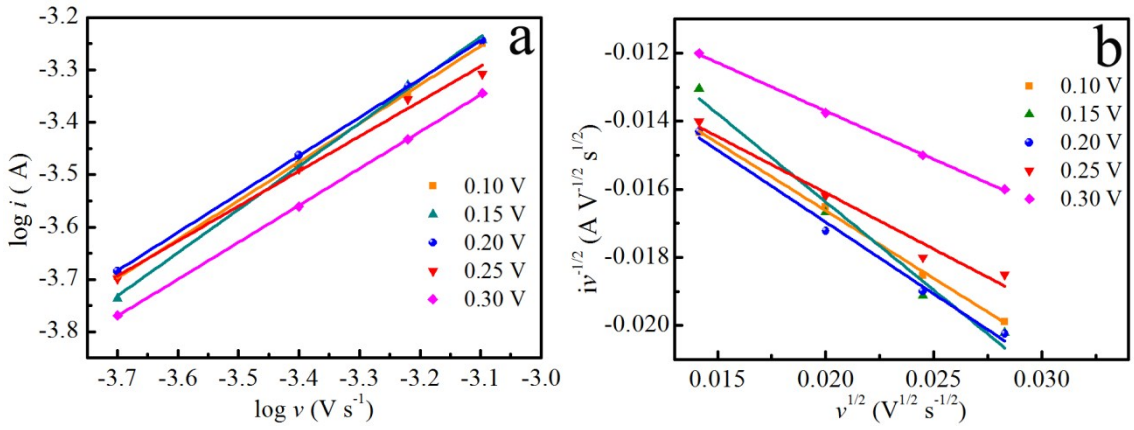

Fig. S5 (a) log *i vs*. log *v* and (b) $iv^{-1/2}$ *vs*. $v^{1/2}$ at different Na-insertion potentials around the reduction peak.

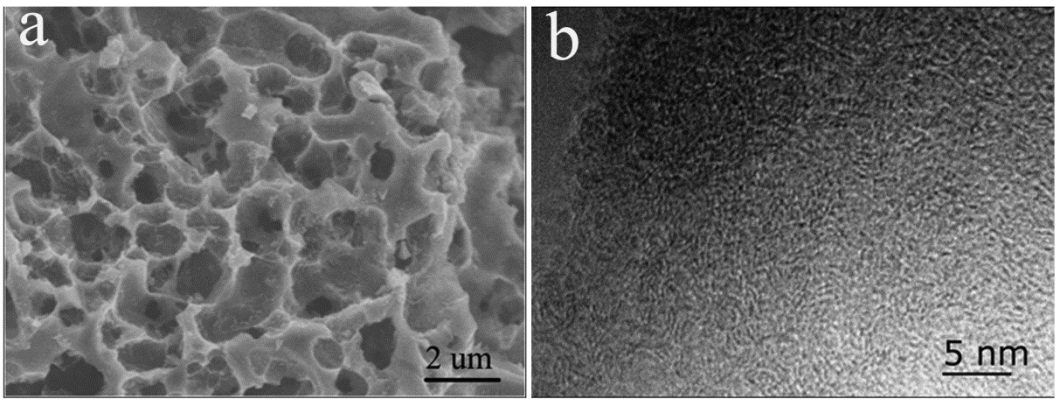

Fig. S6 SEM and HRTEM images of PSC.

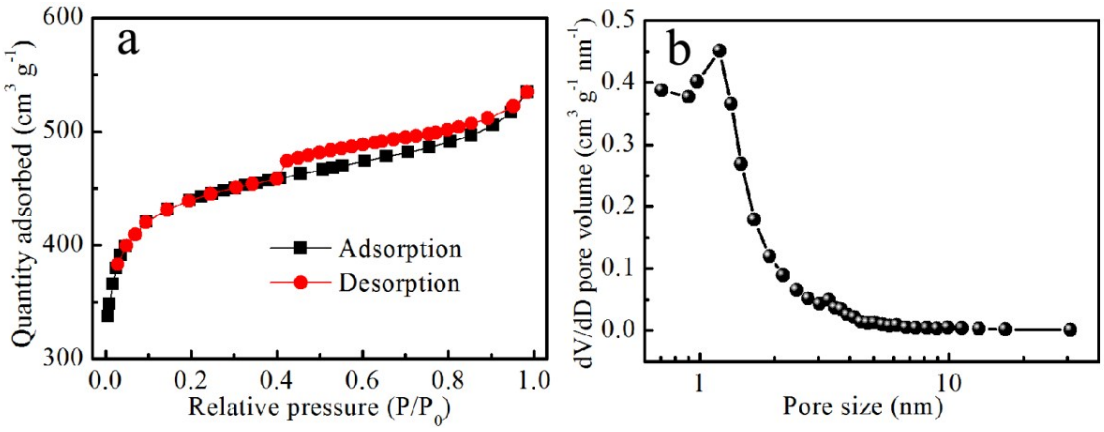

Fig. S7. (a) Nitrogen adsorption-desorption isotherm and (b) Pore size distribution data through the BJH method of PSC.

Figure S7a indicates the Nitrogen adsorption-desorption isotherm of PSC, while Figure S7b indicates its pore size distribution (obtained by BJH method). The typical I/IV-type isotherms could be observed for the PSC specimen, which possesses sizable porosity and specific surface areas. Specifically, the BET surface area is 1900.5 m^2 g^{-1} and total pore volume is 0.86 cm^3 g^{-1} with an average pore diameter of 1.94 nm.

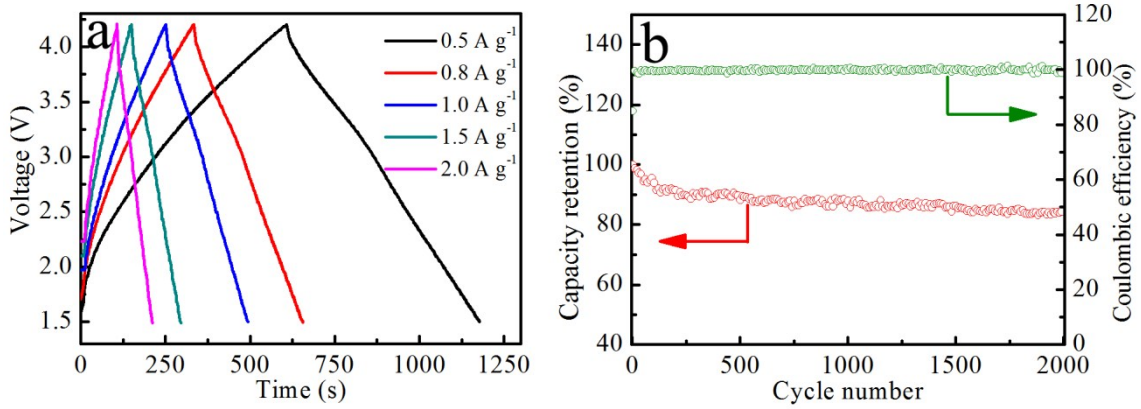

Fig. S8 Electrochemical performance of the Na/PSC half-cell within a voltage window of 1.5 - 4.2 V. (a) Galvanostatic charge-discharge curves at various densities. (b) Plots of specific capacity versus cycle number at 0.5 A g^{-1} for 2000 cycles.

Table S1. Electrochemical performance of different NTO materials.

Reference	Type of material	Specific capacity (mAh g^{-1})	Cycle performance
This work	NTO@CNT	100 mAh g^{-1} at 3.4 A g^{-1}	100 mAh g^{-1} after 1000 cycles at 1.7 A g^{-1}
1	Single crystalline NTO rods	85 mAh g^{-1} at 0.085 A g^{-1}	55 mAh g^{-1} after 20 cycles at 0.085 A g^{-1}
2	NTO nanotubes	--	125.8 mAh g^{-1} after 60 cycles at 0.017 A g^{-1}
3	NTO nanotubes	60 mAh g^{-1} at 0.5 A g^{-1}	105 mAh g^{-1} after 50 cycles at 0.017 A g^{-1}
4	NTO/C composites	79.5 mAh g^{-1} at 0.89 A g^{-1}	72.8 mAh g^{-1} after 100 cycles at 0.89 A g^{-1}
5	NTO nanotubes-assembled 3D spider-web architecture	100 mAh g^{-1} at 3.0 A g^{-1}	107 mAh g^{-1} after 500 cycles at 0.5 A g^{-1}

1 W. Wang, C. Yu, Y. Liu, J. Hou, H. Zhu and S. Jiao, *RSC Advances*, 2013, **3**, 1041.

2 L. Zhao, L. Qi and H. Wang, *J. Power Sources*, 2013, **242**, 597.

3 J. Yin, L. Qi and H. Wang, *ACS Appl. Mater. Interfaces*, 2012, **4**, 2762.

4 Z. C. Yan, L. Li, H. B. Shu, X. K. Yang, H. Wang, J. L. Tan, Q. Zhou, Z. F. Huang and X. Y. Wang, *J. Power Sources*, 2015, **274**, 8.

5 Y. Zhang, L. Guo and S. Yang, *Chem. Commun.*, 2014, **50**, 14029.